Examination of Leakage and End Effects in a Linear Synchronous Motor for Vertical Transportation by Means of Finite Element Computation

M. Platen and G. Henneberger

***Abstract*—This paper presents an examination of leakage and end effects in a linear synchronous motor used as a drive for a vertical transportation system. By means of finite element computation the effect of a skewing of the motor on the propulsion force is calculated. The influence of horizontal displacements of the secondary caused by movements of the cage is investigated. Furthermore, the effect of a reduction of the air gap as well as the influence of the end effects of the linear motor on the propulsion force are examined. The calculated propulsion force is compared to measurements taken from a model of the hoisting system.**

***Index Terms*—Finite element method, forces, linear synchronous motor.**

I. Introduction

A BASIC demand for a vertical transportation system is the smoothness of motion of the drive. As linear drives are direct drives by definition, this requires a small ripple of the propulsion force of the motor. Furthermore, the normal force of the motor has to be very small. Therefore, a detailed evaluation of the propulsion force and of the normal force is essential for a reliable layout of a linear motor for a vertical transportation system.

The objective of this paper is the examination of the propulsion force of the investigated linear motor as a function of leakage effects and the skewing of the motor. In a first step the motor is calculated without a skewing of the permanent magnets. Then calculations are carried out for a layout with skewed permanent magnets to analyze the effect of the skewing on the propulsion force.

Furthermore, for the motor with skewed permanent magnets the influence of a displacement of the secondary in normal direction is investigated. The maximum displacement in normal direction $\Delta y = 4$ mm is given by the tolerances of the guide of the hoisting system.

One way to improve the efficiency of a motor is a reduction of the air gap. The basic layout of the motor allows for a mechanical air gap of 7 mm on each side of the stator, which includes a safety margin for mechanical tolerances of 3 mm. Therefore, a layout with a mechanical air gap reduced to two times 5 mm is investigated.

Manuscript received June 5, 2000.

The authors are with the Department of Electrical Machines, Aachen Institute of Technology (RWTH), Germany (e-mail: {platen; henneberger}@iem.rwth-aachen.de).

Publisher Item Identifier S 0018-9464(01)07902-X.

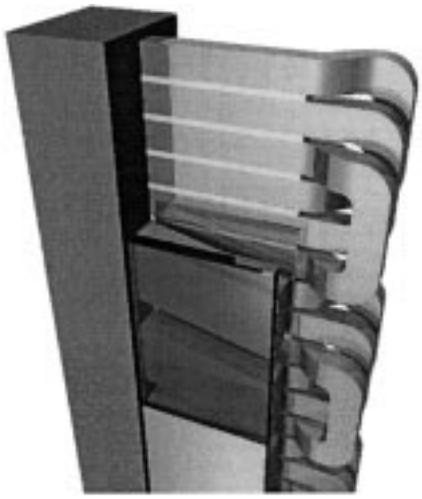

Fig. 1. The geometry of the linear motor.

Finally the end effects of the linear motor, i.e., the influence of the leakage at the top end and at the bottom end of the iron core on the propulsion force, are examined.

II. Structure of the Motor

In principle, various types of linear motors can be used as a direct drive for a vertical transportation system. In comparison to induction motors for example, the power density of synchronous motors is quite independent of the air gap. Therefore, the examined linear synchronous motor is a good choice for a vertical transportation system with its wide and furthermore variable air gap [1]–[3].

Fig. 1 shows the geometry of the motor. The coils of the primary side are fixed to the hoistway by means of holding stems and cast resin. The secondary side of the motor consists of two sets of permanent magnets situated on both sides of the stator coils. The permanent magnets and the iron yokes are fastened to the cage.

The motor has two peculiarities: First, the coils are constructed ironless to minimize the normal forces of the motor. Second, the permanent magnets of the secondary are skewed to reduce the ripple of the propulsion force.

The primary coils are fed with field-oriented sinusoidal current so that the stator field has an offset of electrical 90° to the exciting field.

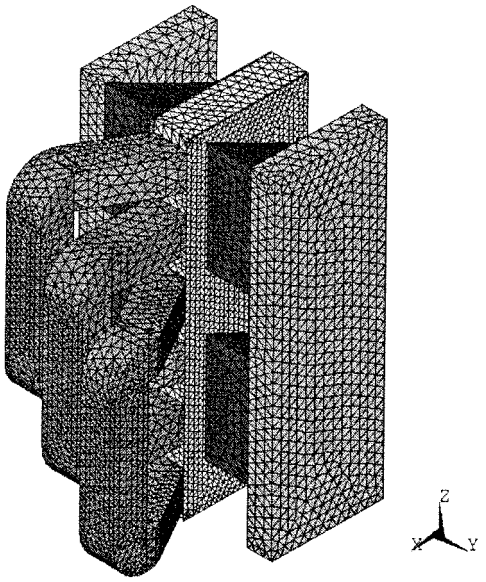

Fig. 2. Mesh of the basic finite element model.

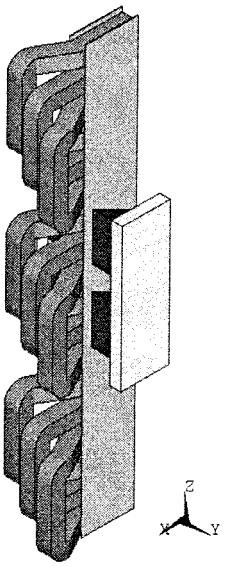

Fig. 3. Finite element model for the examination of end effects.

III. Calculation Method

A. Finite Element Computation

For the shape variation of the motor and for the calculation of the propulsion force and the normal force three-dimensional static finite element computation is used [4]. Because of the slow variation of the electromagnetic properties in the linear motor a time-step finite element computation is not necessary.

The basic finite element model for the motor with skewed permanent magnets is depicted in Fig. 2. Because of the symmetry of the motor only half the length of the core and two pole pitches τ_p of the motor are modeled. The model consists of 500.000 elements. For the examination of the end effects of the linear motor a finite element model with six pole pitches is calculated. Fig. 3 shows a surface plot of this model.

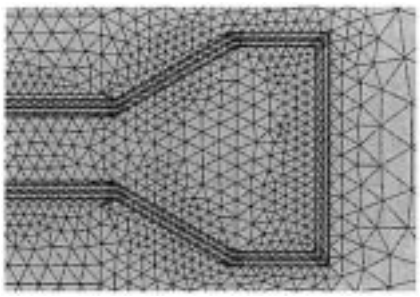

Fig. 4. Detail of the finite element mesh in a cross-section in the xy-plane.

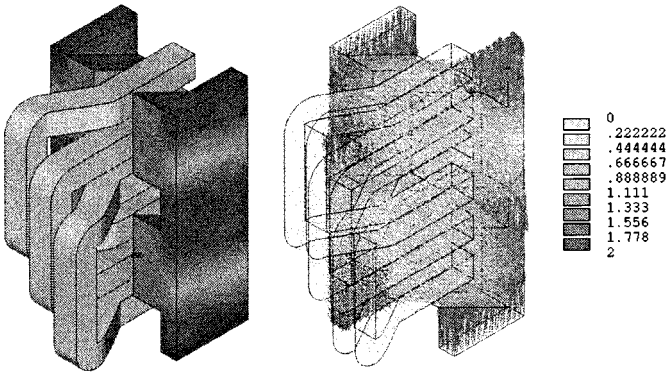

Fig. 5. Absolute value and field shape of the flux density as a surface plot (Tesla).

To calculate the motor for different electrical angles the permanent magnets are shifted in positive z-direction. The electrical angle β is defined as

$$\beta = \frac{z}{\tau_p} \cdot 180^\circ. \tag{1}$$

Calculations have been carried out for 12 different positions of the secondary relative to the stator coils.

As normal forces in an ironless motor are caused by leakage, a detailed modeling of the coils and the coil ends is necessary. Fig. 4 shows a detail of the finite element mesh in a cross-section of the coil in the xy-plane.

Fig. 5 shows the absolute value of the flux density and the field shape of the motor with skewed permanent magnets for rated load as a surface plot.

B. Force Calculation

To derive the propulsion force and the normal force of the motor from the finite element computation the Maxwell stress method is employed.

The equation

$$\vec{F} = \frac{1}{\mu} \cdot \oint_S \mathbf{T}\, d\vec{S} \tag{2}$$

with the Maxwell stress tensor

$$\mathbf{T} = \begin{pmatrix} B_x^2 - \frac{1}{2}|B|^2 & B_x \cdot B_y & B_x \cdot B_z \\ B_y \cdot B_x & B_y^2 - \frac{1}{2}|B|^2 & B_y \cdot B_z \\ B_z \cdot B_x & B_z \cdot B_y & B_z^2 - \frac{1}{2}|B|^2 \end{pmatrix} \tag{3}$$

calculates the force on a solid from the distribution of the flux density $\vec{B}$ on a closed envelope surface S around that solid.

To compute the forces between primary and secondary sectional planes are laid in the air gaps and around the coil ends of

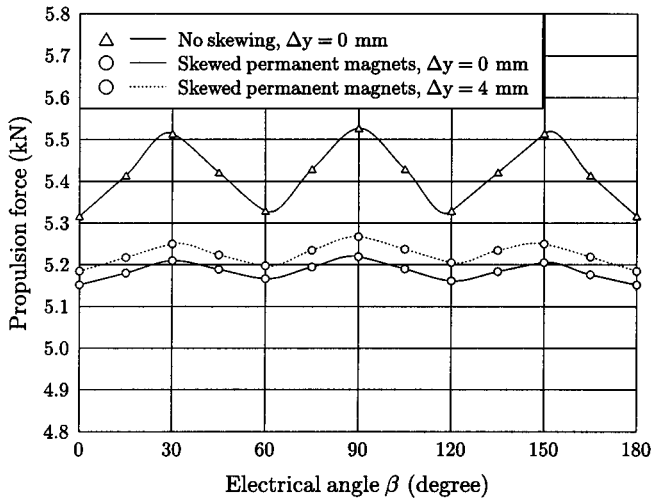

Fig. 6. Calculated propulsion force per meter length of the secondary for a motor without skewing and for a motor with skewed permanent magnets.

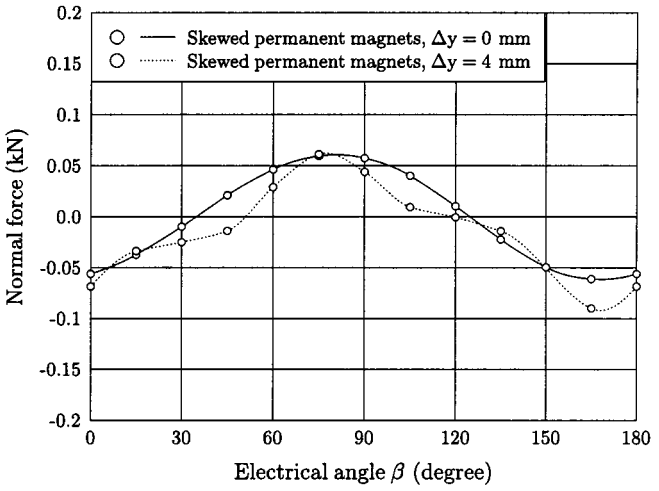

Fig. 7. Calculated normal force per meter length of the secondary for the motor with skewed permanent magnets.

the motor. The Maxwell stress method is quite sensitive to the choice of the sectional plane in the air gap. Therefore, three sets of sections are evaluated and the average of the results is found.

As for zero current condition there are no propulsion forces or normal forces in the examined geometry, the forces calculated for this condition are caused by discretization errors and numerical errors. To reduce the effect of these errors on the Maxwell stress tensor for each position the results for the currentless model are subtracted from the forces calculated for rated load. Due to the large attractive forces between the permanent magnets of the two motor sides this correction has a slight influence on the normal force but no effect on the calculated propulsion force.

IV. Results

A. Skewing of the Permanent Magnets

As a small ripple of the propulsion force is a basic requirement for the examined application, the skewing of the motor is an obvious step to optimize the drive. For the layout with skewed permanent magnets a skewing about one third of a pole pitch is modeled. Fig. 6 shows the propulsion force per meter length of the secondary over one pole pitch for the layout without skewing and for the layout with skewed permanent magnets.

The propulsion force reaches its maximum values at positions $\beta = 30° + n \cdot 60°$, where two coils fed with $\sqrt{3}/2$ rated current are in the heights of the permanent magnets. The force ripple for the layout without skewing is approximately 4% of the mean value. The skewing of the permanent magnets reduces the ripple of the propulsion force to well below 2% of the mean value. This achievement comes along with a reduction of the mean value of the propulsion force of about 5%. All further examinations are carried out for the motor with skewed permanent magnets.

B. Horizontal Displacement of the Secondary

The mechanical tolerance of the hoisting system allows for a remarkable horizontal displacement of the secondary side in y-direction.

The propulsion force of the motor with skewed permanent magnets for maximum displacement in y-direction $\Delta y = 4$ mm is depicted in Fig. 6. The slight increase of the propulsion force for maximum displacement compared to the calculations for zero displacement is caused by the leakage in the air gap. The horizontal displacement has no noteworthy influence on the force ripple.

The influence of a horizontal displacement of the secondary on the normal force has also been investigated for the motor with skewed permanent magnets. Fig. 7 shows the calculated normal force per meter length of the secondary over one pole pitch. For zero displacement $\Delta y = 0$ mm as well as for maximum displacement $\Delta y = 4$ mm the normal force reaches less than 2% of the propulsion force. Even taking into account the numerical tolerances of the normal force calculation caused by the large attractive forces between the permanent magnets the normal force has no influence on the driving performance of the motor [5].

C. Variation of the Air Gap

Fig. 8 shows the calculated propulsion force per meter length of the secondary for the basic layout of the motor with a mechanical air gap of 7 mm and for a motor with a mechanical air gap reduced to 5 mm. The air gap reduction of two times 2% mm results in an increase of the propulsion force of the motor of about 7%.

Due to the reduced leakage the smaller air gap causes a slightly higher force ripple. Nevertheless, a reducing of the mechanical air gap is an effective way to improve the efficiency of the motor.

D. End Effects of the Linear Motor

In general, end effects of linear motors only have to be considered for quite short motors. For the examined motor the finite element computation reveals that the leakage at the top and bottom end of the iron cores leads to a reduction of the propulsion force of approximately 10% for the top and bottom pole pitch.

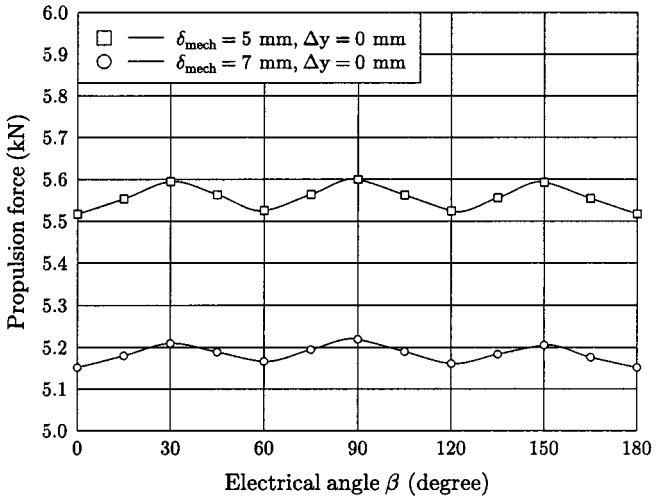

Fig. 8. Calculated propulsion force per meter length of the secondary for a motor with a mechanical air gap of 5 mm and for a motor with a mechanical air gap of 7 mm.

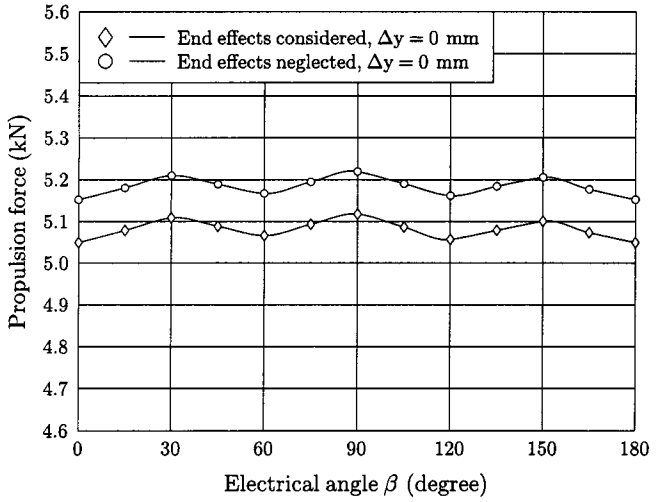

Fig. 9. Calculated propulsion force for a motor with a secondary length of 1 meter with the end effects taken into account and with the end effects neglected.

Fig. 9 shows the calculated propulsion force for a motor with a secondary length of 1 meter. The consideration of the end effects results in a reduction of the propulsion force of about 2%.

V. Comparison to Test Results

Static measurements of the propulsion force have been taken from a model of a hoisting system. The hoisting system is equipped with the examined linear synchronous motor with skewed permanent magnets. Fig. 10 shows the calculated propulsion force and the measured values for a secondary length of 1 meter for zero displacement $\Delta y = 0$ mm. The remarkable mean variation of the measured values taken from several sets of coils can be put down to manufacturing tolerances of the handmade coils.

The measured values are on average 2% smaller than the results of the finite element computation. Furthermore, the measured force ripple and the calculated force ripple show good correspondence.

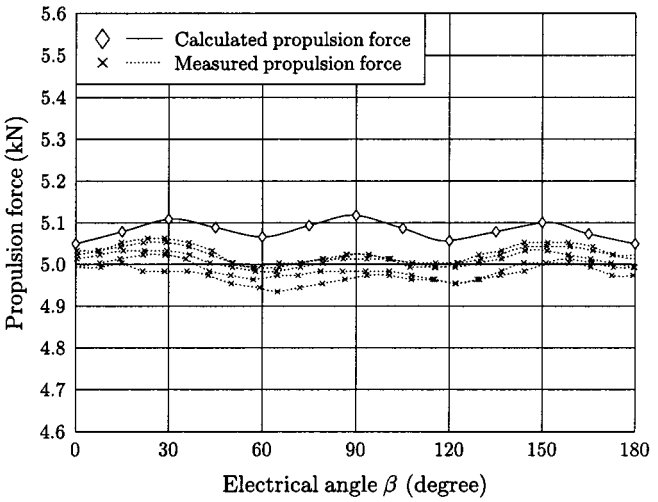

Fig. 10. Calculated and measured propulsion force for a motor with a secondary length of 1 meter for zero displacement $\Delta y = 0$ mm.

VI. Conclusions

In this work the propulsion force of the examined linear synchronous motor has been investigated as a function of leakage effects and the skewing of the motor.

By a skewing of the permanent magnets about one third of a pole pitch the ripple of the propulsion force can be reduced to well below 2% of the mean value, which is less than half the ripple of the nonskewed motor.

A horizontal displacement of the secondary side relative to the stator coils causes a slight increase of the propulsion force but has no influence on the force ripple.

For the examined motor, a decrease of the mechanical airgap of 2 mm results in an increase of the propulsion force of about 7%. Therefore, a reduction of the mechanical air gap is an effective way to improve the efficiency of the motor.

The leakage at the top and bottom end of the iron core leads to a reduction of the propulsion force of approximately 10% for the top and bottom pole pitch.

Based on these results the design of linear motors of the described type for various payloads will be easily possible.

References

[1] T. Koseki, S. Sone, M. Watada, S. Torii, and D. Ebihara, "Transient currents and thrust of a linear synchromous motor with permanent magnets for vertical transportation," in *Symposium on Power Electronics, Electrical Drives, Advanced Electrical Motors*, 1994, pp. 231–236.

[2] V. Gore, R. J. Cruise, and C. F. Landy, "Economic considerations of linear synchronous motors in the South African mining industry," *Linear Drives for Ind. App. (LDIA'98)*, pp. 86–89, 1998.

[3] M. Miyatake, N. Ishikawa, T. Koseki, and S. Sone, "Experimental and operational study on vertical transportation system driven by a linear synchronous motor using permanent magnets," *Linear Drives for Ind. App. LDIA'95*, pp. 73–76, 1995.

[4] D. Albertz, "Entwicklung numerischer Verfahren zur Berechnung und Auslegung elektromagnetischer Schienenbremssysteme," Ph.D. dissertation, RWTH Aachen, 1999.

[5] M. Platen, W. Evers, and G. Henneberger, "A linear synchronous motor for a vertical transportation system -numerical calculations and test results," in *8th Int. IGTE Symp. Numerical Field Calculation in Elec. Eng.*, 1998, pp. 571–574.